HIGHER-ORDER RELAXATION SCHEMES FOR HYPERBOLIC SYSTEMS OF CONSERVATION LAWS

Mapundi K. Banda

Fachbereich Mathematik, TU Darmstadt,
64289 Darmstadt, Germany

banda@mathematik.tu-darmstadt.de

Mohammed Seaïd

Fachbereich Mathematik, TU Darmstadt,
64289 Darmstadt, Germany

seaid@mathematik.tu-darmstadt.de

We present a higher order generalization for relaxation methods in the framework presented by Jin and Xin in [9]. The schemes employ general higher order integration for spatial discretization and higher order implicit-explicit (IMEX) schemes or Total Variation diminishing (TVD) Runge-Kutta schemes for time integration of relaxing or relaxed schemes, respectively, for time integration. Numerical experiments are performed on various test problems, in particular, the Burger's and Euler equations of inviscid gas dynamics in both one and two space dimensions. In addition, uniform convergence with respect to the relaxation parameter is demonstrated.

Keywords: Relaxation methods; hyperbolic systems; higher order upwind schemes; Runge-Kutta methods.

AMS Subject Classification: 35L65, 76M12, 65L06, 76P05

1. Introduction

It is the goal of this paper to construct higher order relaxation schemes for the one dimensional hyperbolic system of conservation laws

$$\begin{aligned} \frac{\partial \mathbf{u}}{\partial t} + \frac{\partial}{\partial x}\mathbf{f}(\mathbf{u}) = 0, \quad x \in \mathbb{R}, \quad t > 0, \\ \mathbf{u}(x,0) = \mathbf{u}_0(x), \quad x \in \mathbb{R}, \end{aligned} \tag{1.1}$$

where $\mathbf{u} \in \mathbb{R}^m$ and the flux function $\mathbf{f}(\mathbf{u}) : \mathbb{R}^m \to \mathbb{R}^m$ is nonlinear. We apply the relaxation method presented in [9] to problem (1.1) whereby we obtain a relaxation system of the form:

$$\begin{aligned} \frac{\partial \mathbf{u}}{\partial t} + \frac{\partial \mathbf{v}}{\partial x} &= 0, \\ \frac{\partial \mathbf{v}}{\partial t} + \mathbf{A}^2 \frac{\partial \mathbf{u}}{\partial x} &= -\frac{1}{\tau}\Big(\mathbf{v} - \mathbf{f}(\mathbf{u})\Big), \\ \mathbf{u}(x,0) = \mathbf{u}_0(x), \quad & \mathbf{v}(x,0) = \mathbf{f}\big(\mathbf{u}_0(x)\big), \end{aligned} \tag{1.2}$$

where $\mathbf{v} \in \mathbb{R}^m$, $\mathbf{A}^2 := \text{diag}\big(a_1^2, \ldots, a_m^2\big) \in \mathbb{R}^{m\times m}$ and τ is the relaxation rate. The relaxation system (1.2) has a typical semilinear structure with the $2m$ linear characteristic variables

$$\mathbf{v} + \mathbf{A}\mathbf{u} \qquad \text{and} \qquad \mathbf{v} - \mathbf{A}\mathbf{u}. \tag{1.3}$$

Hence we have replaced a nonlinear system by a semi-linear system with the main advantage that it can be solved numerically without introducing Riemann solvers. Moreover, it has been shown analytically, see for example [4,14,16,17], that solutions to (1.2) approach solutions to the original problem (1.1) if the subcharacteristic condition

$$\frac{|\lambda|}{a_i} \leq 1, \qquad i = 1, \ldots m, \tag{1.4}$$

is satisfied for every eigenvalue λ of $\mathbf{f}'(\mathbf{u})$.

The relaxation system as defined above were first introduced in [9]. There a first order upwind scheme and a second order MUSCL scheme was used for the space discretization and second order implicit-explicit (IMEX) Runge-Kutta scheme for the time integration. See also other approaches in [5,7,11,21] and the references cited therein. In [9] second order schemes were developed.

In this paper we follow the same idea and extend it to higher order. A derivation of the higher order schemes will be presented. This demonstrates that the accuracy of relaxation schemes can be increased by using higher order reconstruction and a sufficiently accurate quadrature rule for the approximation of fluxes. To achieve this a third-order extension is presented. A non-linear limiting augments the reconstruction in order to prevent oscillations. This is all achieved without sacrificing the simplicity and structure of the original scheme in [9]. Further it will be demonstrated that the accuracy of the scheme is maintained uniformly for different values of τ. This clearly demonstrates the fact that relaxation schemes can be used as a means of constructing simple alternative high order schemes for relaxed systems ($\tau = 0$) or for hyperbolic conservation laws of the form (1.1) in general.

The rest of the paper is organized as follows: Section 2 presents an overview of the basic ideas of relaxation schemes, special attention is paid to the first and second order schemes. Section 3 is devoted to the construction of high order relaxation schemes with a more detailed formulation of a third order scheme. Extension to the two-dimensional problem is discussed in section 4. Numerical results for the Burger's and Euler equations of gas dynamics are reported in section 5. Section 6 contains concluding remarks.

2. The Relaxation Schemes: A Brief Overview

Relaxation schemes are in fact a combination of non-oscillatory upwind space discretization and an implicit-explicit time integration of the resulting semi-discrete system, see for instance [9,16,17]. The fully discrete system of the equations (1.2) is referred to as a *relaxing system* while that of the limiting system as the relaxation rate tends to zero, $\tau \to 0$, is called a *relaxed system.*

To discretize the system of equations (1.2) we assume, for simplicity, an equally spaced grid with grid space $\Delta x := x_{i+\frac{1}{2}} - x_{i-\frac{1}{2}}$ and a uniform time step $\Delta t := t_{n+1} - t_n$. We use the notation

$$\omega^n_{i+\frac{1}{2}} := \omega(x_{i+\frac{1}{2}}, t_n) \quad \text{and} \quad \omega^n_i := \frac{1}{\Delta x}\int_{x_{i-\frac{1}{2}}}^{x_{i+\frac{1}{2}}} \omega(x, t_n)dx,$$

to denote the point-value and the approximate cell-average of the function ω at $x = x_{i+\frac{1}{2}}$, $t = t_n$; and $x = x_i$, $t = t_n$, respectively.

We define the following finite differences

$$\mathcal{D}_x\omega_i := \frac{\omega_{i+\frac{1}{2}} - \omega_{i-\frac{1}{2}}}{\Delta x}. \tag{2.5}$$

Then, a semi-discrete approximation for the system of equations (1.2) can be written as

$$\begin{aligned} \frac{d\mathbf{u}_i}{dt} + \mathcal{D}_x\mathbf{v}_i &= 0, \\ \frac{d\mathbf{v}_i}{dt} + \mathbf{A}^2\mathcal{D}_x\mathbf{u}_i &= -\frac{1}{\tau}\Big(\mathbf{v}_i - \mathbf{f}(\mathbf{u}_i)\Big). \end{aligned} \tag{2.6}$$

Notice that, the space and time discretizations are treated separately using the method of lines. Any approximation for the numerical fluxes in (2.5) should be accompanied by an ODE solver for (2.6) of the same order of accuracy. In this section we give a brief overview of the first and second order relaxing systems as presented in [9].

2.1. *First order relaxation scheme*

A first order upwind scheme is applied to the characteristic variables (1.3) in order to obtain the numerical fluxes in (2.5) for the k-th component by

$$(v + a_k u)_{i+\frac{1}{2}} = (v + a_k u)_i, \qquad (v - a_k u)_{i+\frac{1}{2}} = (v - a_k u)_{i+1}.$$

to obtain

$$\begin{aligned} u_{i+\frac{1}{2}} &:= \frac{u_i + u_{i+1}}{2} - \frac{v_{i+1} - v_i}{2a_k}, \\ v_{i+\frac{1}{2}} &:= \frac{v_i + v_{i+1}}{2} - a_k\frac{u_{i+1} - u_i}{2}. \end{aligned} \tag{2.7}$$

To integrate in time the equations (2.6), a first order implicit-explicit splitting given by the usual Butcher tables is used

$$\begin{array}{c|c} 0 & 0 \\ \hline & 1 \end{array} \qquad\qquad \begin{array}{c|c} 1 & 1 \\ \hline & 1 \end{array} \tag{2.8}$$

where the left and right tables represent the explicit and implicit Runge-Kutta schemes, respectively. Hence, the implementation of the first order relaxation algorithm to solve (1.1) is carried out in simple steps as follows:

Given $\{u_i^n, v_i^n\}$, $\{u_i^{n+1}, v_i^{n+1}\}$ are computed by

$$\begin{aligned} u_i^* &= u_i^n, \\ v_i^* &= v_i^n - \frac{\Delta t}{\tau}\Big(v_i^* - \mathbf{f}(u_i^*)\Big); \\ u_i^{(1)} &= u_i^* - \Delta t \mathcal{D}_x v_i^*, \\ v_i^{(1)} &= v_i^* - \Delta t \mathbf{A}^2 \mathcal{D}_x u_i^*; \\ u_i^{n+1} &= u_i^{(1)}, \\ v_i^{n+1} &= v_i^{(1)}. \end{aligned} \tag{2.9}$$

When $\tau \longrightarrow 0$, equations (2.9) reduce to the so called relaxed scheme

$$\begin{aligned} u_i^{(1)} &= u_i^n - \Delta t \mathcal{D}_x v_i^n \Big|_{v_i^n = \mathbf{f}(u_i^n)}, \\ u_i^{n+1} &= u_i^{(1)}. \end{aligned} \tag{2.10}$$

Note that, the relaxed scheme (2.10) is the first order explicit scheme given by the left table in (2.8), applied to the original system (1.1). The finite difference, $\mathcal{D}_x$, is defined as in (2.5) by projecting the numerical flux $v_{i+\frac{1}{2}}$ into the local equilibrium $\mathbf{f}_{i+\frac{1}{2}} := \mathbf{f}(u_{i+\frac{1}{2}})$ using (2.7). A similar scheme has also been attributed to Rusanov in [13].

2.2. *Second order relaxation scheme*

For the second order scheme, we use the MUSCL method presented in [19] for the discretization along the characteristic variables (1.3). This method yields the semi-discrete system (2.6), where the numerical fluxes for the k-th component are

$$\begin{aligned} u_{i+\frac{1}{2}} &:= \frac{u_i + u_{i+1}}{2} - \frac{v_{i+1} - v_i}{2a_k} + \frac{\sigma_i^+ + \sigma_{i+1}^-}{4a_k}, \\ v_{i+\frac{1}{2}} &:= \frac{v_i + v_{i+1}}{2} - a_k \frac{u_{i+1} - u_i}{2} + \frac{\sigma_i^+ - \sigma_{i+1}^-}{4}. \end{aligned} \tag{2.11}$$

We use Sweby's notation to define the slopes of $v \pm a_k u$ by

$$\sigma_i^\pm = \big(v_{i+1} \pm a_k u_{i+1} - v_i \mp a_k u_i\big)\phi(\theta_i^\pm), \qquad \theta_i^\pm = \frac{v_i \pm a_k u_i - v_{i-1} \mp a_k u_{i-1}}{v_{i+1} \pm a_k u_{i+1} - v_i \mp a_k u_i},$$

and ϕ is a slope limiter function. The simplest choice of a slope limiter is the so-called minmod limiter,

$$\phi(\theta) = \max(0, \min(1, \theta)).$$

A sharper Van-Leer limiter may also be used which is given by [19],

$$\phi(\theta) = \frac{|\theta| + \theta}{1 + |\theta|}.$$

Note that if we set the slopes $\sigma_i^{\pm} = 0$ or $\phi = 0$, the equations (2.11) reduce to the first order scheme (2.7).

With a similar piecewise implicit-explicit reconstruction as before, the second order Runge-Kutta scheme presented in [10] is given. Its corresponding Butcher double tables are

$$\begin{array}{c|cc} 0 & 0 & 0 \\ 1 & 1 & 0 \\ \hline & \frac{1}{2} & \frac{1}{2} \end{array} \qquad\qquad \begin{array}{c|cc} -1 & -1 & 0 \\ 2 & 1 & 1 \\ \hline & \frac{1}{2} & \frac{1}{2} \end{array} \tag{2.12}$$

Consequently, we can formulate the second order relaxation scheme to integrate (1.2) as follows: Given $\{u_i^n, v_i^n\}$, $\{u_i^{n+1}, v_i^{n+1}\}$ are computed by

$$\begin{aligned}
u_i^* &= u_i^n, \\
v_i^* &= v_i^n + \frac{\Delta t}{\tau}\Big(v_i^* - \mathbf{f}(u_i^*)\Big); \\
u_i^{(1)} &= u_i^* - \Delta t \mathcal{D}_x v_i^*, \\
v_i^{(1)} &= v_i^* - \Delta t \mathbf{A}^2 \mathcal{D}_x u_i^*; \\
u_i^{**} &= u_i^{(1)}, \\
v_i^{**} &= v_i^{(1)} - \frac{\Delta t}{\tau}\Big(v_i^{**} - \mathbf{f}(u_i^{**})\Big) - \frac{2\Delta t}{\tau}\Big(v_i^* - \mathbf{f}(u_i^*)\Big); \\
u_i^{(2)} &= u_i^{**} - \Delta t \mathcal{D}_x v_i^{**}, \\
v_i^{(2)} &= v_i^{**} - \Delta t \mathbf{A}^2 \mathcal{D}_x u_i^{**}; \\
u_i^{n+1} &= \frac{1}{2}(u_i^n + u_i^{(2)}), \\
v_i^{n+1} &= \frac{1}{2}(v_i^n + v_i^{(2)}).
\end{aligned} \tag{2.13}$$

It was shown in [9], the variables v_i^* and v_i^{**} in (2.13) approximate the local equilibrium $\mathbf{f}(u_i^*)$ and $\mathbf{f}(u_i^{**})$, respectively when $\tau \longrightarrow 0$. Therefore, a second order relaxed scheme is obtained, based on the left explicit table in (2.12), as

$$\begin{aligned}
u_i^{(1)} &= u_i^n - \Delta t \mathcal{D}_x v_i^n \Big|_{v_i^n = \mathbf{f}(u_i^n)}, \\
u_i^{(2)} &= u_i^{(1)} - \Delta t \mathcal{D}_x v_i^{(1)} \Big|_{v_i^{(1)} = \mathbf{f}(u_i^{(1)})}, \\
u_i^{n+1} &= \frac{1}{2}(u_i^n + u_i^{(2)}).
\end{aligned} \tag{2.14}$$

It is worth remarking that, using these schemes neither linear algebraic equation nor nonlinear source terms can arise. In addition both first and second order relaxation schemes are stable independent of τ, so that the choice of Δt is based only on the usual CFL condition

$$\text{CFL} := \max_{1\leq k\leq m}\{a_k^2\}\frac{\Delta t}{\Delta x} \leq 1.$$

Note also that the time-discretization in the limit when $\tau \longrightarrow 0$ converges to the formally TVD Runge-Kutta schemes given by Shu and Osher in [6], also referred to as Strong Stability-Preserving (SSP) time discretization methods in [8]. We further remark that different choices of $a_k, k \in \{1,\ldots,m\}$ can be taken. In [9] several choices have been highlighted. Other plausible choices have been used in the numerical experiments in this paper and will be discussed below.

3. Third- and Higher-Order Relaxation Schemes

We generalize the relaxation schemes so that higher order schemes can be used. The idea is to define an interpolating polynomial which is used in the MUSCL-type formulation above. Using this formulation the fluxes at the cell boundaries can be derived.

To generalize the relaxation schemes we will first modify our notation slightly: Using the discretization introduced in section 2 we consider a cell in the domain Ω which we denote $\mathcal{I}_i = [x_{i-\frac{1}{2}}, x_{i+\frac{1}{2}}]$ containing the gridpoint x_i . We denote an interpolating polynomial defined on cell $\mathcal{I}_i$ by $p_i(x,t)$. Thus the k-th component of the solution is reconstructed by piecewise polynomials as:

$$\tilde{u}(x,t) = \sum_i p_i(x,t;\mathbf{u})\chi_i(x). \tag{3.15}$$

where χ_i is a characteristic function defined on cell $\mathcal{I}_i$. The values of $\tilde{u}$ at the cell boundary point between cells $\mathcal{I}_i$ and $\mathcal{I}_{i+1}$, $x_{i+\frac{1}{2}}$, are denoted as:

$$u_k^+(x_{i+\frac{1}{2}};\mathbf{u}) = p_{i+1}(x_{i+\frac{1}{2}};\mathbf{u}) \qquad \text{and} \qquad u_k^-(x_{i+\frac{1}{2}};\mathbf{u}) = p_i(x_{i+\frac{1}{2}};\mathbf{u}).$$

Now and henceforth, the subscript k will be dropped. It is clear that in the first and second order schemes presented above the following reconstructions were used:

$$\begin{aligned} p_i(x;\mathbf{u}) &= u_i, \\ p_i(x;\mathbf{u}) &= u_i + (u_x)_i(x - x_i), \end{aligned}$$

where u_x is the slope of u. The reconstruction at $x_{i-\frac{1}{2}}$ is defined analogously.

Using this description it is possible to define higher order relaxation schemes using higher order reconstructions. For the presentation of this scheme here the Central Weighted Essentially Non-Oscillatory (CWENO) reconstruction in [12] which is also the Compact Central scheme reconstruction [15] will be used. Other reconstructions have been used but the results thereof will not be reported here.

The CWENO reconstruction is defined as below, for more details refer to [12,15]. Let

$$p_i(x;\mathbf{u}) = w_L P_L(x) + w_R P_R(x) + w_C P_C(x), \tag{3.16}$$

where, for $l, j \in \{L, R, C\}$

$$w_l = \frac{\alpha_l}{\displaystyle\sum_j \alpha_j}, \quad \sum_l w_l = 1, \quad \alpha_l = \frac{c_l}{(\varepsilon + IS_l)^p}, \quad c_L = c_R = \frac{1}{4}, \quad c_C = \frac{1}{2}, \tag{3.17}$$

$$IS_L = (u_i - u_{i-1})^2, \qquad IS_R = (u_{i+1} - u_i)^2,$$

$$IS_C = \frac{13}{3}(u_{i+1} - 2u_i + u_{i-1})^2 + \frac{1}{4}(u_{i+1} - u_{i-1})^2,$$

$$P_L(x) = u_i + \frac{u_i - u_{i-1}}{\Delta x}(x - x_i), \qquad P_R(x) = u_i + \frac{u_{i+1} - u_i}{\Delta x}(x - x_i),$$

$$P_C(x) = u_i - \frac{1}{12}(u_{i+1} - 2u_i + u_{i-1}) + \frac{u_{i+1} - u_{i-1}}{2\Delta x}(x - x_i) + \frac{(u_{i+1} - 2u_i + u_{i-1})}{(\Delta x)^2}(x - x_i)^2.$$

The constant ε guarantees that the denominator does not vanish and is empirically taken to be 10^{-6} [15]. Likewise the value of p is chosen to provide the highest accuracy in smooth areas and ensure the non-oscillatory nature of the solution near the discontinuities and is selected to be $p = 2$.

With this background we can now reconstruct the characteristic variables as follows:

$$\begin{aligned}
(v + au)_{i+\frac{1}{2}} &= (v + au)^-_{i+\frac{1}{2}} = p_i(x_{i+\frac{1}{2}}; \mathbf{v} + a\mathbf{u}), \\
(v - au)_{i+\frac{1}{2}} &= (v - au)^+_{i+\frac{1}{2}} = p_{i+1}(x_{i+\frac{1}{2}}; \mathbf{v} - a\mathbf{u}).
\end{aligned}$$

Hence:

$$\begin{aligned}
u_{i+\frac{1}{2}} &= \frac{1}{2a}\Big(p_i(x_{i+\frac{1}{2}}; \mathbf{v} + a\mathbf{u}) - p_{i+1}(x_{i+\frac{1}{2}}; \mathbf{v} - a\mathbf{u})\Big), \\
v_{i+\frac{1}{2}} &= \frac{1}{2}\Big(p_i(x_{i+\frac{1}{2}}; \mathbf{v} + a\mathbf{u}) + p_{i+1}(x_{i+\frac{1}{2}}; \mathbf{v} - a\mathbf{u})\Big).
\end{aligned}$$

For completeness we write down the explicit expressions of the flux variables below:

$$\begin{aligned}
v_{i+\frac{1}{2}} &= \frac{1}{2}\Big(p_i(x_{i+\frac{1}{2}}; \mathbf{v} + a\mathbf{u}) + p_{i+1}(x_{i+\frac{1}{2}}; \mathbf{v} - a\mathbf{u})\Big) \\
&= \frac{1}{2}\Bigg\{ w_L^+\Big[(v + au)_i + \frac{1}{2}\Big((v + au)_i - (v + au)_{i-1}\Big)\Big] + \\
&\quad w_R^+\Big[(v + au)_i + \frac{1}{2}\Big((v + au)_{i+1} - (v + au)_i\Big)\Big] + \\
&\quad w_C^+\Big[(v + au)_i - \frac{1}{12}\Big((v + au)_{i+1} - 2(v + au)_i + (v + au)_{i-1}\Big) + \\
&\quad \frac{1}{4}\Big((v + au)_{i+1} - (v + au)_{i-1}\Big) +
\end{aligned}$$

$$
\begin{aligned}
&\frac{1}{4}\Big((v+au)_{i+1}-2(v+au)_i+(v+au)_{i-1}\Big)\Big]+\\
&w_L^-\Big[(v-au)_{i+1}+\frac{1}{2}\Big((v-au)_{i+1}-(v-au)_i\Big)\Big]+\\
&w_R^-\Big[(v-au)_{i+1}+\frac{1}{2}\Big((v-au)_{i+2}-(v-au)_{i+1}\Big)\Big]+\\
&w_C^-\Big[(v-au)_{i+1}-\frac{1}{12}\Big((v-au)_{i+2}-2(v-au)_{i+1}+(v-au)_i\Big)+\\
&\frac{1}{4}\Big((v-au)_{i+2}-(v-au)_i\Big)+\\
&\frac{1}{4}\Big((v-au)_{i+2}-2(v-au)_{i+1}+(v-au)_i\Big)\Big]\Big\},
\end{aligned}
$$

where, for $l, j \in \{L, R, C\}$

$$
w_l^{\pm}=\frac{\alpha_l^{\pm}}{\sum_j \alpha_j^{\pm}},\quad \sum_l w_l^{\pm}=1,\quad \alpha_l^{\pm}=\frac{c_l}{(\varepsilon+IS_l)^p},\quad c_L=c_R=\frac{1}{4},\quad c_C=\frac{1}{2},\tag{3.18}
$$

$$
IS_L^{\pm}=\Big((v\pm au)_i-(v\pm au)_{i-1}\Big)^2,\quad IS_R^{\pm}=\Big((v\pm au)_{i+1}-(v\pm au)_i\Big)^2
$$

$$
\begin{aligned}
IS_C^{\pm}=&\frac{13}{3}\Big((v\pm au)_{i+1}-2(v\pm au)_i+(v\pm au)_{i-1}\Big)^2+\\
&\frac{1}{4}\Big((v\pm au)_{i+1}-(v\pm au)_{i-1}\Big)^2.
\end{aligned}
$$

The expression for $u_{i+\frac{1}{2}}$ can be derived analogously. Therefore, we obtain the following expressions for $u_{i+\frac{1}{2}}$ and analogously for $v_{i+\frac{1}{2}}$:

$$
\begin{aligned}
u_{i+\frac{1}{2}} &:= \frac{u_i+u_{i+1}}{2}-\frac{v_{i+1}-v_i}{2a_k}+\frac{\sigma_i^+ + \sigma_{i+1}^-}{4a_k}+\frac{\phi_i^+ - \phi_{i+1}^-}{4a_k},\\
v_{i+\frac{1}{2}} &:= \frac{v_i+v_{i+1}}{2}-a_k\frac{u_{i+1}-u_i}{2}+\frac{\sigma_i^+ - \sigma_{i+1}^-}{4}+\frac{\phi_i^+ + \phi_{i+1}^-}{4},
\end{aligned}
$$

where

$$
\begin{aligned}
\sigma_i^{\pm} &= w_L^{\pm}\Big((v\pm au)_i-(v\pm au)_{i-1}\Big)+w_R^{\pm}\Big((v\pm au)_{i+1}-(v\pm au)_i\Big)+\\
&\quad \frac{w_C^{\pm}}{2}\Big((v\pm au)_{i+1}-(v\pm au)_{i-1}\Big),\\
\phi_i^{\pm} &= \frac{w_C^{\pm}}{3}\Big((v\pm au)_{i+1}-2(v\pm au)_i+(v\pm au)_{i-1}\Big).
\end{aligned}
$$

We close by pointing out that in this higher order scheme we approximate $f(u)_i$ using the fourth-order Simpson quadrature rule as opposed to the Midpoint Rule which was used in the first and second order cases i.e.

$$
\mathbf{f}(u)_i=\frac{1}{6}\Big[\mathbf{f}(\tilde{u}_{i+\frac{1}{2}})+4\mathbf{f}(\tilde{u}_i)+\mathbf{f}(\tilde{u}_{i-\frac{1}{2}})\Big],
$$

where the reconstruction given above is used:

$$\tilde{u}_{i+\frac{1}{2}} = u^-_{i+\frac{1}{2}}, \qquad \tilde{u}_i = p_i(x_i;\mathbf{u}), \qquad \tilde{u}_{i-\frac{1}{2}} = u^+_{i-\frac{1}{2}}.$$

Thus for the CWENO reconstruction we obtain the following approximations:

$$\begin{aligned}
\tilde{u}_{i+\frac{1}{2}} &= w_L P_L(x_{i+\frac{1}{2}}) + w_R P_R(x_{i+\frac{1}{2}}) + w_C P_C(x_{i+\frac{1}{2}}),\\
\tilde{u}_i &= w_L P_L(x_i) + w_R P_R(x_i) + w_C P_C(x_i),\\
\tilde{u}_{i-\frac{1}{2}} &= w_L P_L(x_{i-\frac{1}{2}}) + w_R P_R(x_{i-\frac{1}{2}}) + w_C P_C(x_{i-\frac{1}{2}}),
\end{aligned} \tag{3.19}$$

with the corresponding weights, w_L, w_R, w_C of the polynomials defined accordingly.

The time integration of the space discretized equations is accomplished by third order Runge-Kutta splitting developed in [2,18], the associated explicit and implicit Butcher tables are

$$\begin{array}{c|ccccc}
0 & 0 & 0 & 0 & 0 & 0\\
\frac{1}{2} & \frac{1}{2} & 0 & 0 & 0 & 0\\
\frac{2}{3} & \frac{11}{18} & \frac{1}{18} & 0 & 0 & 0\\
\frac{1}{2} & \frac{5}{6} & -\frac{5}{6} & \frac{1}{2} & 0 & 0\\
1 & \frac{1}{4} & \frac{7}{4} & \frac{3}{4} & -\frac{7}{4} & 0\\
\hline
 & \frac{1}{4} & \frac{7}{4} & \frac{3}{4} & -\frac{7}{4} & 0
\end{array}
\qquad
\begin{array}{c|ccccc}
0 & 0 & 0 & 0 & 0 & 0\\
\frac{1}{2} & 0 & \frac{1}{2} & 0 & 0 & 0\\
\frac{2}{3} & 0 & \frac{1}{6} & \frac{1}{2} & 0 & 0\\
\frac{1}{2} & 0 & -\frac{1}{2} & \frac{1}{2} & \frac{1}{2} & 0\\
1 & 0 & \frac{3}{2} & -\frac{3}{2} & \frac{1}{2} & \frac{1}{2}\\
\hline
 & 0 & \frac{3}{2} & -\frac{3}{2} & \frac{1}{2} & \frac{1}{2}
\end{array} \tag{3.20}$$

This procedure can be easily formulated similarly as in (2.9) and (2.13). Moreover, as in the case of first and second order schemes, this third order scheme is stable independently of τ under the CFL condition

$$\mathrm{CFL} := \max_{1\le k\le m}\left(\frac{\Delta t}{h}, a_k^2\frac{\Delta t}{\Delta x}\right) \le 1.$$

Obviously, when $\tau \longrightarrow 0$, this scheme leads to the relaxed scheme for the limit equations, which is based on the explicit table in (3.20).

4. Extension to Multidimensional Problems

Let us consider the two-dimensional hyperbolic system of conservation laws

$$\begin{aligned}
\frac{\partial \mathbf{u}}{\partial t} + \frac{\partial}{\partial x}\mathbf{f}(\mathbf{u}) + \frac{\partial}{\partial y}\mathbf{g}(\mathbf{u}) = \mathbf{0}, \quad (x,y)\in\mathbb{R}^2, \quad t>0,\\
\mathbf{u}(x,y,0) = \mathbf{u}_0(x,y), \quad (x,y)\in\mathbb{R}^2,
\end{aligned} \tag{4.22}$$

where $u \in \mathbb{R}^m$, $\mathbf{f}(\mathbf{u})$ and $\mathbf{g}(\mathbf{u})$ are nonlinear flux functions in $\mathbb{R}^m$. The associated relaxation system reads

$$\begin{aligned}
\frac{\partial \mathbf{u}}{\partial t} + \frac{\partial}{\partial x}\mathbf{v} + \frac{\partial \mathbf{w}}{\partial y} &= \mathbf{0},\\
\frac{\partial \mathbf{v}}{\partial t} + \mathbf{A}^2\frac{\partial \mathbf{u}}{\partial x} &= -\frac{1}{\tau}\big(\mathbf{v} - \mathbf{f}(\mathbf{u})\big),\\
\frac{\partial \mathbf{w}}{\partial t} + \mathbf{B}^2\frac{\partial \mathbf{u}}{\partial y} &= -\frac{1}{\tau}\big(\mathbf{w} - \mathbf{g}(\mathbf{u})\big).
\end{aligned} \tag{4.23}$$

Consequently, in the limit $\tau \longrightarrow 0$, system (4.23) approaches the original system (4.22) by the local equilibrium

$$\mathbf{v} = \mathbf{f}(\mathbf{u}) \quad \text{and} \quad \mathbf{w} = \mathbf{g}(\mathbf{u}).$$

Moreover, the elements of $\mathbf{A}$ and $\mathbf{B}$ are chosen according to the subcharacteristic condition[4,14,16,17]

$$\frac{|\lambda_k|}{a_k} + \frac{|\mu_k|}{b_k} \leq 1, \qquad k = 1, 2, \ldots, m, \tag{4.24}$$

where λ_k and μ_k are the k-th eigenvalues of the Jacobians of $\mathbf{f}(\mathbf{u})$ and $\mathbf{g}(\mathbf{u})$, respectively. For the space discretization of the equations (4.23), we cover Ω with rectangular cells $\mathcal{C}_{i,j} := [x_{i-\frac{1}{2}}, x_{i+\frac{1}{2}}] \times [y_{j-\frac{1}{2}}, y_{j+\frac{1}{2}}]$ of uniform sizes Δx and Δy. The cells, $\mathcal{C}_{i,j}$, are centered at $(x_i = i\Delta x, y_j = j\Delta y)$. We use the notations $\omega_{i\pm\frac{1}{2},j}(t) := \omega(x_{i\pm\frac{1}{2}}, y_j, t)$, $\quad \omega_{i,j\pm\frac{1}{2}}(t) := \omega(x_i, y_{j\pm\frac{1}{2}}, t)$ and

$$\omega_{i,j}(t) := \frac{1}{\Delta x}\frac{1}{\Delta y}\int_{x_{i-\frac{1}{2}}}^{x_{i+\frac{1}{2}}}\int_{y_{j-\frac{1}{2}}}^{y_{i+\frac{1}{2}}} \omega(x, y, t)dxdy,$$

to denote the point-values and the approximate cell-average of ω at $(x_{i\pm\frac{1}{2}}, y_j, t)$, $(x_i, y_{j\pm\frac{1}{2}}, t)$, and (x_i, y_j, t), respectively. We define the following finite differences

$$\mathcal{D}_x\omega_{i,j} := \frac{\omega_{i+\frac{1}{2},j} - \omega_{i-\frac{1}{2},j}}{\Delta x}, \qquad \mathcal{D}_y\omega_{i,j} := \frac{\omega_{i,j+\frac{1}{2}} - \omega_{i,j-\frac{1}{2}}}{\Delta y}.$$

Then, the semi-discrete approximation of (4.23) is

$$\begin{aligned}
\frac{d\mathbf{u}_{i,j}}{dt} + \mathcal{D}_x\mathbf{v}_{i,j} + \mathcal{D}_y\mathbf{w}_{i,j} &= \mathbf{0}, \\
\frac{d\mathbf{v}_{i,j}}{dt} + \mathbf{A}^2\mathcal{D}_x\mathbf{u}_{i,j} &= -\frac{1}{\tau}\left(\mathbf{v}_{i,j} - \mathbf{f}(\mathbf{u})_{i,j}\right), \\
\frac{d\mathbf{u}_{i,j}}{dt} + \mathbf{B}^2\mathcal{D}_y\mathbf{u}_{i,j} &= -\frac{1}{\tau}\left(\mathbf{w}_{i,j} - \mathbf{g}(\mathbf{u})_{i,j}\right),
\end{aligned} \tag{4.25}$$

The approximate solution is reconstructed by a piecewise polynomial over the grid points as

$$\tilde{u}(x, y, t) = \sum_{i,j} \mathcal{P}_{i,j}(x, y; \mathbf{u})\chi_{i,j}(x, y), \qquad \chi_{i,j} = \mathbb{1}_{\mathcal{C}_{i,j}}, \tag{4.26}$$

where $\mathcal{P}_{i,j}$ are polynomials defined in $\mathcal{C}_{i,j}$ reconstructed "dimension by dimension" as

$$\mathcal{P}_{i,j}(x, y; \mathbf{u}) = \mathcal{P}_i(x; \mathbf{u}) + \mathcal{P}_j(y; \mathbf{u}).$$

In the following we formulate the x-direction polynomial $\mathcal{P}_i(x; \mathbf{u})$, the formulation of $\mathcal{P}_j(y; \mathbf{u})$ can be done analogously. Hence

$$\mathcal{P}_i(x; \mathbf{u}) = \omega_L P_L(x) + \omega_R P_R(x) + \omega_C P_C(x),$$

where the weights ω_l, $l \in \{L, R, C\}$ are the same as in (3.17) with

$$IS_L = (u_{i,j} - u_{i-1,j})^2, \qquad IS_R = (u_{i+1,j} - u_{i,j})^2,$$

$$IS_C = \frac{13}{3}(u_{i+1,j} - 2u_{i,j} + u_{i-1,j})^2 + \frac{1}{4}(u_{i+1,j} - u_{i-1,j})^2,$$

$$P_L(x) = \frac{u_{i,j}}{2} + \frac{u_{i,j} - u_{i-1,j}}{\Delta x}(x - x_i), \qquad P_R(x) = \frac{u_{i,j}}{2} + \frac{u_{i+1,j} - u_{i,j}}{\Delta x}(x - x_i),$$

$$\begin{aligned} P_C(x) = \frac{u_{i,j}}{2} - \frac{1}{24}(u_{i+1,j} - 2u_{i,j} + u_{i-1,j}) - \frac{1}{24}(u_{i,j+1} - 2u_{i,j} + u_{i,j-1}) + \\ \frac{u_{i+1,j} - u_{i-1,j}}{2(\Delta x)}(x - x_i) + \frac{(u_{i+1,j} - 2u_{i,j} + u_{i-1,j})}{(\Delta x)^2}(x - x_i)^2. \end{aligned}$$

We can now discretize the characteristic variables (1.3) as follows

$$\begin{aligned} (v + a_k u)_{i+\frac{1}{2},j} &= \mathcal{P}_i(x_{i+\frac{1}{2}}; v + a_k v), \qquad (v - a_k u)_{i+\frac{1}{2},j} = \mathcal{P}_{i+1}(x_{i+\frac{1}{2}}; v - a_k u); \\ (w + b_k u)_{i,j+\frac{1}{2}} &= \mathcal{P}_j(y_{j+\frac{1}{2}}; w + b_k u), \qquad (w - b_k u)_{i,j+\frac{1}{2}} = \mathcal{P}_{j+1}(y_{j+\frac{1}{2}}; w - b_k u). \end{aligned}$$

Recall that u_k, v_k, w_k, a_k and b_k are the k-th ($k = 1, \ldots, m$) components of $\mathbf{u}$, $\mathbf{v}$, $\mathbf{w}$, $\mathbf{A}$ and $\mathbf{B}$ respectively. Hence

$$\begin{aligned} u_{i+\frac{1}{2},j} &= \frac{1}{2a_k}\left(\mathcal{P}_i(x_{i+\frac{1}{2}}; \mathbf{u} + \mathbf{A}\mathbf{u}) - \mathcal{P}_{i+1}(x_{i+\frac{1}{2}}; \mathbf{v} - \mathbf{A}\mathbf{u})\right), \\ v_{i+\frac{1}{2},j} &= \frac{1}{2}\left(\mathcal{P}_i(x_{i+\frac{1}{2}}; \mathbf{v} + \mathbf{A}\mathbf{u}) + \mathcal{P}_{i+1}(x_{i+\frac{1}{2}}; \mathbf{v} - \mathbf{A}\mathbf{u})\right); \\ u_{i,j+\frac{1}{2}} &= \frac{1}{2b_k}\left(\mathcal{P}_j(y_{j+\frac{1}{2}}; \mathbf{w} + \mathbf{B}\mathbf{u}) - \mathcal{P}_{j+1}(y_{j+\frac{1}{2}}; \mathbf{w} - \mathbf{B}\mathbf{u})\right), \\ w_{i,j+\frac{1}{2}} &= \frac{1}{2}\left(\mathcal{P}_j(y_{j+\frac{1}{2}}; \mathbf{w} + \mathbf{B}\mathbf{u}) + \mathcal{P}_{j+1}(y_{j+\frac{1}{2}}; \mathbf{w} - \mathbf{B}\mathbf{u})\right). \end{aligned}$$

Therefore, we obtain the following expressions for the numerical fluxes in (4.25)

$$\begin{aligned} u_{i+\frac{1}{2},j} &= \frac{u_{i,j} + u_{i+1,j}}{2} - \frac{v_{i+1,j} - v_{i,j}}{2a_k} + \frac{\sigma^{x,+}_{i,j} + \sigma^{x,-}_{i+1,j}}{4a_k} + \frac{\phi^{x,+}_{i,j} - \phi^{x,-}_{i+1,j}}{4a_k}, \\ v_{i+\frac{1}{2},j} &= \frac{v_{i,j} + v_{i+1,j}}{2} - a_k\frac{u_{i+1,j} - u_{i,j}}{2} + \frac{\sigma^{x,+}_{i,j} - \sigma^{x,-}_{i+1,j}}{4} + \frac{\phi^{x,+}_{i,j} + \phi^{x,-}_{i+1,j}}{4}; \\ u_{i,j+\frac{1}{2}} &= \frac{u_{i,j} + u_{i,j+1}}{2} - \frac{w_{i,j+1} - w_{i,j}}{2b_k} + \frac{\sigma^{y,+}_{i,j} + \sigma^{y,-}_{i,j+1}}{4b_k} + \frac{\phi^{y,+}_{i,j} - \phi^{y,-}_{i,j+1}}{4b_k}, \\ w_{i,j+\frac{1}{2}} &= \frac{w_{i,j} + w_{i+1,j}}{2} - b_k\frac{u_{i,j+1} - u_{i,j}}{2} + \frac{\sigma^{y,+}_{i,j} - \sigma^{y,-}_{i,j+1}}{4} + \frac{\phi^{y,+}_{i,j} + \phi^{y,-}_{i,j+1}}{4}, \end{aligned}$$

where $\sigma^{x,\pm}_{i,j}$, $\sigma^{y,\pm}_{i,j}$ are defined as

$$\begin{aligned} \sigma^{x,\pm}_{i,j} &= \omega^{\pm}_L\left((v \pm a_k u)_{i,j} - (v \pm a_k u)_{i-1,j}\right) + \omega^{\pm}_R\left((v \pm a_k u)_{i+1,j} - (v \pm a_k u)_{i,j}\right) \\ &\quad + \frac{\omega^{\pm}_C}{2}\left((v \pm a_k u)_{i+1,j} - (u \pm a_k u)_{i-1,j}\right), \\ \phi^{x,\pm}_{i,j} &= \frac{\omega^{\pm}_C}{3}\left((v \pm a_k u)_{i+1,j} - 2(v \pm a_k u)_{i,j} + (v \pm a_u)_{i-1,j}\right) \\ &\quad - \frac{\omega^{\pm}_C}{6}\left((v \pm a_k u)_{i,j+1} - 2(v \pm a_k u)_{i,j} + (v \pm a_k u)_{i,j-1}\right), \end{aligned}$$

$$
\begin{aligned}
\sigma_{i,j}^{y,\pm} &= \omega_L^{\pm}\left((w \pm b_k u)_{i,j} - (w \pm b_k u)_{i,j-1}\right) + \omega_R^{\pm}\left((w \pm b_k u)_{i,j+1} - (w \pm b_k u)_{i,j}\right) \\
&\quad + \frac{\omega_C^{\pm}}{2}\left((w \pm b_k u)_{i,j+1} - (w \pm b_k u)_{i,j-1}\right) \\
\phi_{i,j}^{y,\pm} &= \frac{\omega_C^{\pm}}{3}\left((w \pm b_k u)_{i,j+1} - 2(w \pm b_k u)_{i,j} + (w \pm b_k u)_{i,j-1}\right) \\
&\quad - \frac{\omega_C^{\pm}}{6}\left((w \pm b_k u)_{i+1,j} - 2(w \pm b_k u)_{i,j} + (w \pm b_k u)_{i-1,j}\right).
\end{aligned}
$$

The weight parameters $\omega_L^{\pm}$, $\omega_R^{\pm}$ and $\omega_C^{\pm}$ for $\sigma_{i,j}^{x,\pm}$ are given in (3.18) with

$$
IS_L^{\pm} = \left((v \pm a_k u)_{i,j} - (v \pm a_k u)_{i-1,j}\right)^2, \quad IS_R^{\pm} = \left((v \pm a_k u)_{i+1,j} - (v \pm a_k u)_{i,j}\right)^2,
$$

$$
\begin{aligned}
IS_C^{\pm} = \frac{13}{3}&\Big((v \pm a_k u)_{i+1,j} - 2(v \pm a_k u)_{i,j} + (v \pm a_k u)_{i-1,j}\Big)^2 + \\
\frac{1}{4}&\Big((v \pm a_k u)_{i+1,j} - (v \pm a_k u)_{i-1,j}\Big)^2.
\end{aligned}
$$

The corresponding weight parameters for $\sigma_{i,j}^{y,\pm}$ are obtained similarly. We close by pointing out that in this higher order scheme we approximate $\mathbf{f}(\mathbf{u})_{i,j}$ and $\mathbf{g}(\mathbf{u})_{i,j}$ in (4.25) using the fourth-order Simpson quadrature rule.

The semi-discrete formulations (4.25) can be rewritten in common ODE notation as

$$
\frac{dY}{dt} = F(Y) - \frac{1}{\tau}G(Y), \tag{4.27}
$$

where the time-dependent vector functions

$$
Y = \begin{pmatrix} \mathbf{u}_{i,j} \\ \mathbf{v}_{i,j} \\ \mathbf{w}_{i,j} \end{pmatrix}, \quad F(Y) = \begin{pmatrix} -\mathcal{D}_x \mathbf{v}_{i,j} - \mathcal{D}_y \mathbf{w}_{i,j} \\ -\mathbf{A}^2 \mathcal{D}_x \mathbf{u}_{i,j} \\ -\mathbf{B}^2 \mathcal{D}_y \mathbf{u}_{i,j} \end{pmatrix}, \qquad G(Y) = \begin{pmatrix} \mathbf{0} \\ \mathbf{v}_{i,j} - \mathbf{f}(\mathbf{u})_{i,j} \\ \mathbf{w}_{i,j} - \mathbf{g}(\mathbf{u})_{i,j} \end{pmatrix}.
$$

We formulate the IMEX scheme for the system (4.27) as

$$
\begin{aligned}
K_l &= Y^n + \Delta t \sum_{m=1}^{l-1} \tilde{a}_{lm} F(K_m) - \frac{\Delta t}{\tau} \sum_{m=1}^{s} a_{lm} G(K_m), \quad l = 1, 2, \ldots, s, \\
Y^{n+1} &= Y^n + \Delta t \sum_{l=1}^{s} \tilde{b}_l F(K_l) - \frac{\Delta t}{\tau} \sum_{l=1}^{s} b_l G(K_l).
\end{aligned} \tag{4.28}
$$

The $s \times s$ matrices $\tilde{A} = (\tilde{a}_{lm})$; $A = (a_{lm})$ and the s-vectors $\tilde{b}$; b are the standard coefficients which characterize the IMEX s-stage Runge-Kutta scheme. They are given by the usual double Butcher tables

$$
\begin{array}{c|ccccc}
0 & 0 & 0 & 0 & 0 & 0 \\
\tilde{c}_2 & \tilde{a}_{21} & 0 & 0 & 0 & 0 \\
\tilde{c}_3 & \tilde{a}_{31} & \tilde{a}_{32} & 0 & 0 & 0 \\
\vdots & \vdots & \vdots & \vdots & \vdots & \vdots \\
\tilde{c}_s & \tilde{a}_{s1} & \tilde{a}_{s2} & \ldots & \tilde{a}_{ss-1} & 0 \\
\hline
 & \tilde{b}_1 & \tilde{b}_2 & \ldots & \tilde{b}_{s-1} & \tilde{b}_s
\end{array}
\qquad
\begin{array}{c|ccccc}
0 & 0 & 0 & 0 & 0 & 0 \\
c_2 & a_{21} & a_{22} & 0 & 0 & 0 \\
c_3 & a_{31} & a_{32} & a_{33} & 0 & 0 \\
\vdots & \vdots & \vdots & \vdots & \vdots & \vdots \\
c_s & a_{s1} & a_{s2} & \ldots & a_{ss-1} & a_{ss} \\
\hline
 & b_1 & b_2 & \ldots & b_{s-1} & b_s
\end{array}
$$

The left and right tables represent the explicit and the implicit Runge-Kutta methods. Then, the implementation of the IMEX algorithm to solve (4.27) is carried out in the following two steps:

(1) For $l = 1, \ldots, s$,

  (a) Evaluate K_l^* as: $K_l^* = Y^n + \Delta t \sum_{m=1}^{l-2} \tilde{a}_{lm} F(K_m) + \Delta t \tilde{a}_{ll-1} F(K_{l-1})$.

  (b) Solve for K_l: $K_l = K_l^* - \dfrac{\Delta t}{\tau} \sum_{m=1}^{l-1} a_{lm} G(K_m) - \dfrac{\Delta t}{\tau} a_{ll} G(K_l)$.

(2) Update Y^{n+1} as: $Y^{n+1} = Y^n + \Delta t \sum_{l=1}^{s} \tilde{b}_l F(K_l) - \dfrac{\Delta t}{\tau} \sum_{l=1}^{s} b_l G(K_l)$.

Notice that, using the relaxation scheme neither linear algebraic equation nor non-linear source terms can arise. In addition the high order relaxation scheme is stable independently of τ, so that the choice of Δt is based only on the usual CFL condition

$$\mathrm{CFL} := \max_{1 \le k \le m} \left(\frac{\Delta t}{h}, a_k^2 \frac{\Delta t}{\Delta x}, b_k^2 \frac{\Delta t}{\Delta y} \right) \le 1, \tag{4.29}$$

where h denotes the maximum cell size, $h = \max(\Delta x, \Delta y)$.

Remark 1.

- To prevent an initial layer as well as a boundary layer, initial conditions and boundary conditions of the equilibrium system are applied (for example, see equation (1.2)).
- The explicit schemes for the limit $\tau \to 0$ are chosen such that TVD schemes are obtained. On the other hand the IMEX schemes are chosen in such a way that the correct asymptotic behaviour of the schemes is captured even on coarse grids.
- The space discretization is obtained based on a CWENO reconstruction of characteristic variables. Other high order reconstructions can be used. Further the numerical fluxes obtained at the cell-edges have a form similar to those of the Central Schemes [13,12] eventhough here more information is integrated into

the nonlinear terms used to define the high order non-oscillatory terms of the scheme. The fluxes obtained from first order reconstruction are identical.

- Further different choices of τ as well as the matrices $\mathbf{A}$ and $\mathbf{B}$ can be made. Some choices we used for the test examples are presented below. For the purposes of just solving the conservation laws we recommend applying the relaxed scheme directly (i.e. $\tau = 0$). We apply different choices of τ for the sake of investigating the asymptotic behaviour and convergence of the schemes in the relaxing regime.
- Introduction of high order integration of the flux does not introduce nonlinear equations. At each stage of the IMEX Runge-Kutta integration the values of $\tilde{\mathbf{u}}$ are computed explicitly and used in the computation of the flux $\mathbf{v}$.

5. Numerical Examples

In this section, we perform some numerical tests with our schemes. We first of all perform accuracy tests on a linear problem. We will consider the relaxed scheme and the relaxing scheme separately. Thereafter, we consider the system of Euler equations describing the flow of an inviscid, compressible fluid.

Table 1. Error-norms for the linear advection problem (5.30) at $t = 1$ using relaxation schemes.

N	Scheme	L^∞-error	Rate	L^1-error	Rate
40	1^{st} order	0.06315	—	0.06047	—
	2^{nd} order	0.04173	—	0.03512	—
	3^{rd} order	0.06217	—	0.03346	—
80	1^{st} order	0.03360	0.91	0.03218	0.91
	2^{nd} order	0.01919	1.12	0.01507	1.22
	3^{rd} order	0.02650	1.23	0.00836	2.00
160	1^{st} order	0.01998	0.75	0.01620	0.99
	2^{nd} order	0.00877	1.13	0.00454	1.73
	3^{rd} order	0.00930	1.51	0.00180	2.21
320	1^{st} order	0.00992	1.01	0.00720	1.17
	2^{nd} order	0.00219	2.00	0.00093	2.28
	3^{rd} order	0.00143	2.70	0.00016	3.46

5.1. *One-dimensional examples*

5.1.1. *Scalar test examples*

Consider the scalar linear hyperbolic equation

$$u_t + u_x = 0, \qquad x \in [0, 2\pi], \tag{5.30}$$

augmented with the initial data, $u(x,0) = \sin x$, and periodic boundary conditions. This problem admits a global classical solution, which was computed at time $t = 1$ with a varying number of grid points, N.

The associated relaxation system to (5.30) is constructed as in (1.2). We choose $a^2 = 1$ and $\tau = 10^{-8}$ in all the computations. In Table 5 we display the errors at $t = 1$ measured in terms of L^∞- and L^1- norms by the difference between the pointvalues of the exact solution and the reconstructed pointvalues of the computed solution. Table 5.1.1 shows similar results for the relaxed schemes. We obtain the expected order of accuracy in both L^∞- and L^1- norms. These results demonstrate clearly the numerical convergence of the relaxation schemes to the relaxed schemes as $\tau \longrightarrow 0$ for this example.

Table 2. Error-norms for the linear advection problem (5.30) at $t = 1$ using relaxed schemes.

N	Scheme	L^∞-error	Rate	L^1-error	Rate
40	1^{st} order	0.05923	—	0.05370	—
	2^{nd} order	0.03271	—	0.02913	—
	3^{rd} order	0.05432	—	0.02531	—
80	1^{st} order	0.03196	0.89	0.02779	0.95
	2^{nd} order	0.01443	1.18	0.01207	1.27
	3^{rd} order	0.02190	1.31	0.00624	2.02
160	1^{st} order	0.01631	0.97	0.01370	1.02
	2^{nd} order	0.00574	1.33	0.00314	1.94
	3^{rd} order	0.00678	1.69	0.00126	2.30
320	1^{st} order	0.00793	1.04	0.00541	1.34
	2^{nd} order	0.00142	2.01	0.00057	2.45
	3^{rd} order	0.00088	2.94	0.00010	3.61

In the next example we consider solutions to the inviscid Burger's equation,

$$u_t + (\frac{u^2}{2})_x = 0, \qquad x \in [0, 2\pi], \tag{5.31}$$

augmented with the smooth initial data, $u(x,0) = 0.5 + \sin(x)$, and periodic boundary conditions. We set $a^2 = 1.23$, $h = 0.01$ and CFL $= 0.123$.

Recall that the unique entropy solution of (5.31) is smooth up to the critical time $t = 1$. In figure 1, we plot the convergence rate versus τ at the pre-shock time $t = 0.5$ when the solution is still smooth. These convergence plots have been obtained by computing the approximate convergence rate between two consecutive mesh refinings in the L^2-norm. A log-scale on the x-axis is used.

As expected all the schemes preserve the order of accuracy for both large and small values of τ. Moreover, for the first and third order schemes the accuracy in u component is uniform with respect to τ. On the other hand, a deterioration of the accuracy on the v component is observed for all schemes. We want to point out

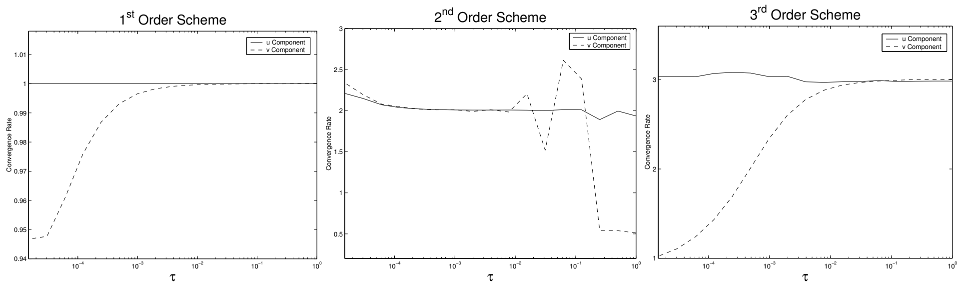

Fig. 1. Convergence rates of the relaxation schemes for Burger's equation.

that we cannot quantify the resolution of the schemes on the v component since an accurate approximation of v can be computed from u in the limit when $\tau \longrightarrow 0$. As expected the third order scheme is remarkably more accurate than other schemes.

5.1.2. *Inviscid Euler equations*

Here we consider the one-dimensional Euler system of gas dynamics,

$$\frac{\partial}{\partial t}\begin{pmatrix}\rho \\ \rho v \\ E\end{pmatrix} + \frac{\partial}{\partial x}\begin{pmatrix}\rho v \\ \rho v^2 + p \\ v(E+p)\end{pmatrix} = 0, \tag{5.32}$$

or simply

$$\frac{\partial \mathbf{u}}{\partial t} + \frac{\partial}{\partial x}\mathbf{f}(\mathbf{u}) = 0, \tag{5.33}$$

where $\mathbf{u} := (\rho, \rho v, E)^T$ and $\mathbf{f}(\mathbf{u}) := \big(\rho v, \rho v^2 + p, v(E+p)\big)^T$, and ρ is the density, v is the velocity, ρv is the momentum, E is the energy and p is the pressure. In addition we require the equation of state $p = (\gamma - 1)(E - \frac{1}{2}\rho v^2)$, where ratio of the specific heats is $\gamma = 1.4$

Based on the formulation (5.33), a relaxation system can be constructed as in (1.2) where $\mathbf{A}^2 = \mathrm{diag}\big(a_1^2, a_2^2, a_3^2\big)$. We define the CFL number as in (4.29). As we have observed, in the previous examples, the third order scheme is in all the cases better than other schemes, we present for this example only results performed with third order relaxation scheme using $\tau = 10^{-8}$. The relaxed results are also not included here, because they overlap those obtained by the relaxation schemes. The following test cases are selected:

Sod shock tube test. The first test is the typical Sod shock tube problem. Its solution consists of a left rarefaction, a contact and right shock [22]. It is formulated by the equations (5.32) augmented by the initial condition

$$\mathbf{u}(x,0) = \begin{cases} (1, 0, 2.5)^T, & \text{if} \quad 0 \le x < 0.5, \\ (0.125, 0, 0.25)^T, & \text{if} \quad 0.5 \le x \le 1. \end{cases}$$

We take $a_1^2 = 1$, $a_2^2 = 1.68$, $a_3^2 = 5.045$, $h = 0.005$ and CFL $= 0.75$. Figure 2 shows the third-order relaxation results with $\tau = 10^{-8}$ at $t = 0.1644$.

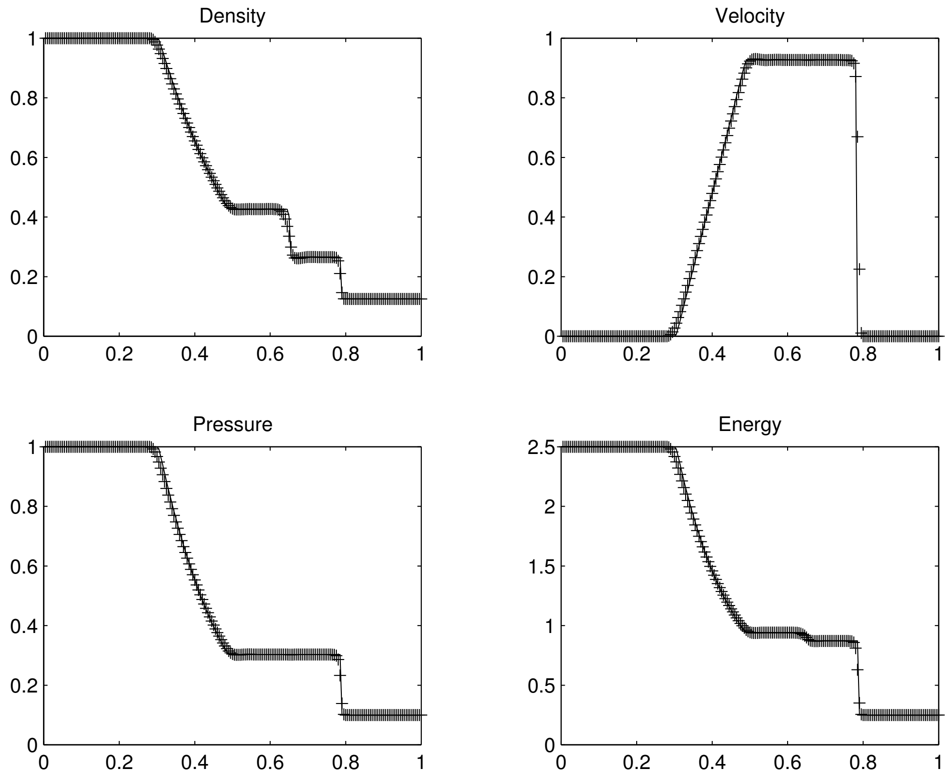

Fig. 2. Relaxation results for Sod shock tube test at $t = 0.1644$.

Lax Shock Tube Test. Our second test is the Lax shock tube test problem [23]. It is mathematically formulated by equations (5.32) subject to the initial data

$$\mathbf{u}(x,0) = \begin{cases} (0.445, 0.311, 8.928)^T, & \text{if} \quad 0 \le x < 0.5, \\ (0.5, 0, 0.4275)^T, & \text{if} \quad 0.5 \le x \le 1. \end{cases}$$

We choose $a_1^2 = 2.4025$, $a_2^2 = 11$, $a_3^2 = 22.2056$, $h = 0.005$ and CFL $= 0.5$. In Figure 3 we present the results obtained by the third-order relaxation scheme with $\tau = 10^{-8}$ at $t = 0.16$.

Interacting Blast Wave Test. Our final test with Euler equations is the interacting blast wave problem characterized by the initial condition [20]

$$\mathbf{u}(x,0) = \begin{cases} (1, 0, 2500)^T, & \text{if} \quad 0 \le x \le 0.1, \\ (1, 0, 0.25)^T, & \text{if} \quad 0.1 < x \le 0.9, \\ (1, 0, 250)^T, & \text{if} \quad 0.9 < x < 1. \end{cases}$$

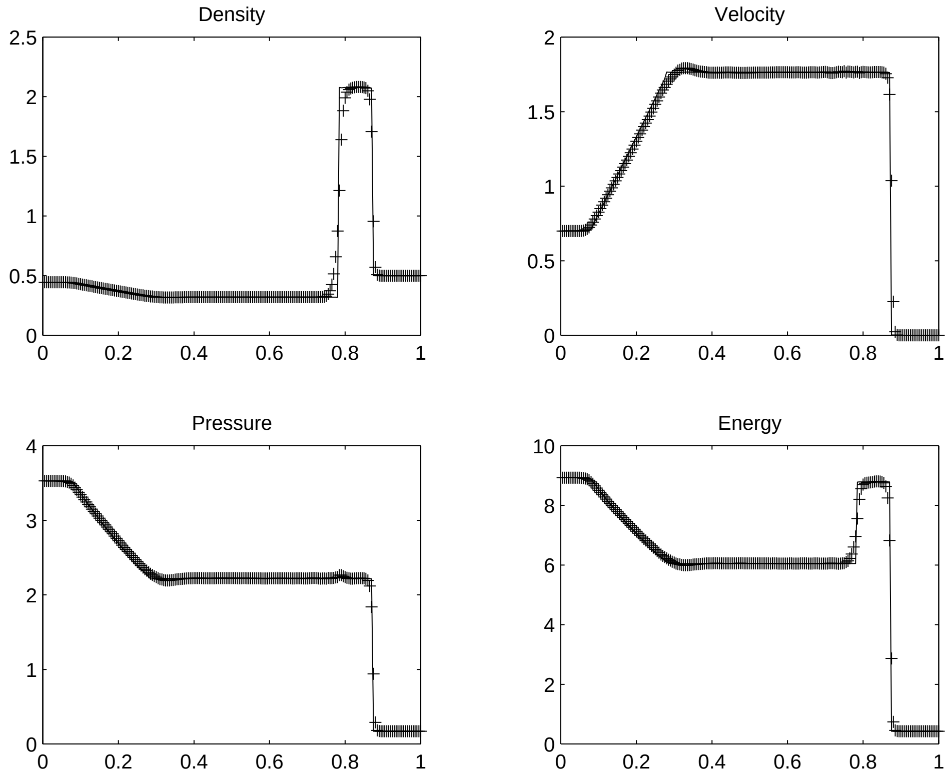

Fig. 3. Relaxation results for Lax shock tube test at $t = 0.16$.

We set $a_1^2 = 32.56$, $a_2^2 = 169$, $a_3^2 = 411.8397$, $h = 0.0025$ and CFL $= 0.25$. Results obtained by the third order relaxation scheme with $\tau = 10^{-8}$ at $t = 0.01$ and $t = 0.038$ are shown in Figure 4 and Figure 5, respectively. The scheme performs very well on the strong shocks in all the examples.

From the above examples one can see that the accurate results are obtained very cheaply. In particular the good results demonstrated for the Euler equations of gas dynamics reveal clearly that the approach has very good potential.

5.2. *Two-dimensional examples*

We present numerical results for some of hyperbolic equations in two space dimensions using our third order extension of the relaxation scheme. We consider both scalar and system of nonlinear equations of conservation laws. In all the computational results presented in this section the relaxation rate τ is set to 10^{-6}.

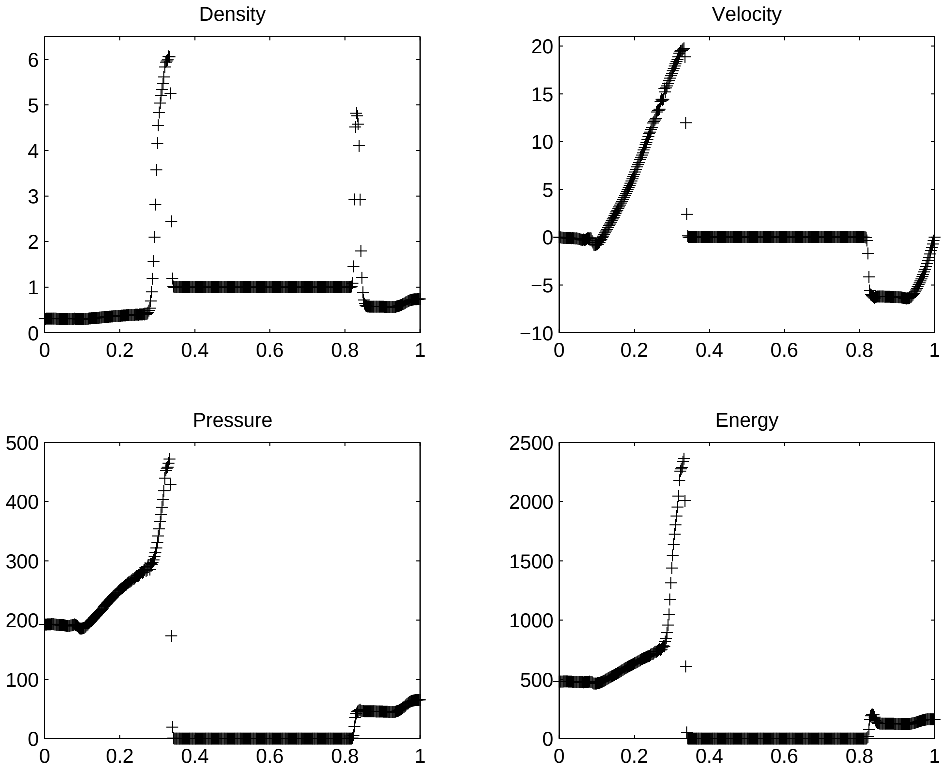

Fig. 4. Relaxation results for interacting Blast wave test at $t = 0.01$.

5.2.1. *Nonlinear scalar example*

We consider the invscid Burger's equation in two space dimensions

$$\begin{aligned} u_t + \left(\frac{u^2}{2}\right)_x + \left(\frac{u^2}{2}\right)_y = 0, \qquad (x, y) \in [0, 1] \times [0, 1], \\ u(x, y, 0) = \sin^2(\pi x) \sin^2(\pi y), \quad (x, y) \in [0, 1] \times [0, 1], \end{aligned} \tag{5.34}$$

augmented with periodic boundary conditions. By setting the flux functions $f(u) = g(u) = u^2/2$, the associated relaxation system to (5.34) can be formulated as in (4.23). We discretize the space domain uniformly into 50×50 gridpoints and we compute the solution using $a^2 = 1$, $b^2 = 1$ and CFL $= 0.87$.

The obtained results are shown in figure 6 at four different times, $t = 1$, 2, 3, and 4. The solutions are completely free of spurious oscillations and the shocks are well resolved by the third order relaxing scheme.

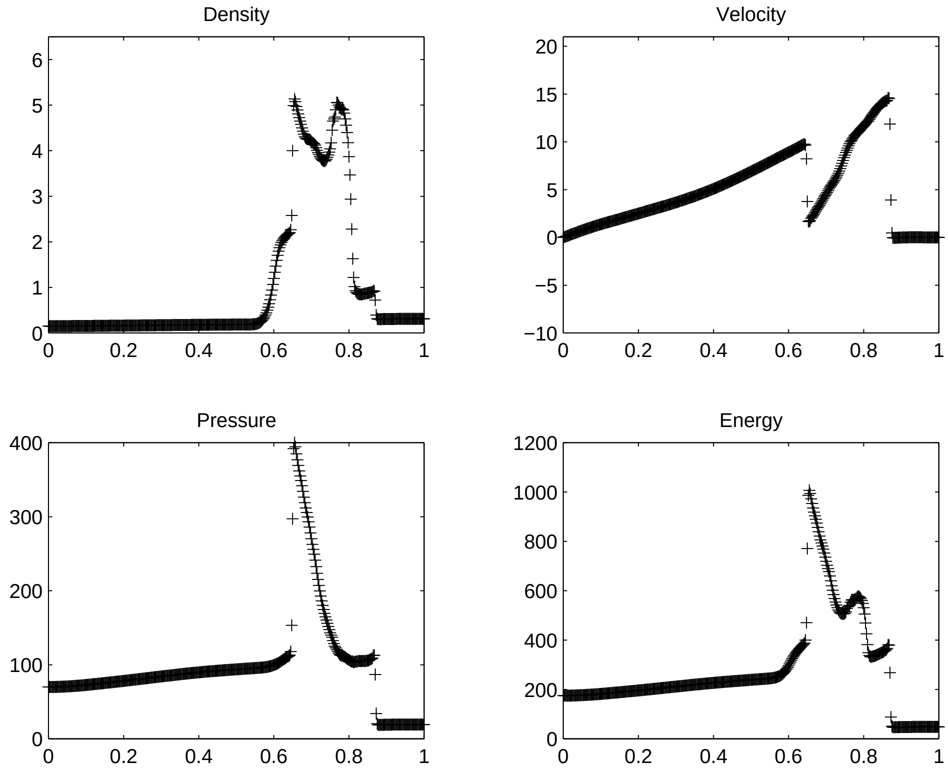

Fig. 5. Relaxation results for interacting Blast wave test at $t = 0.038$.

5.2.2. *Nonlinear system of inviscid Euler equations*

The Euler equations for an ideal gas in two space dimensions are given by the system (4.22) where

$$\mathbf{u} = \begin{pmatrix} \rho \\ \rho u \\ \rho v \\ E \end{pmatrix}, \quad \mathbf{f}(\mathbf{u}) = \begin{pmatrix} \rho u \\ \rho u^2 + p \\ \rho uv \\ u(E+p) \end{pmatrix}, \quad \mathbf{g}(\mathbf{u}) = \begin{pmatrix} \rho v \\ \rho uv \\ \rho v^2 + p \\ v(E+p) \end{pmatrix}. \tag{5.35}$$

In (5.35), ρ is the density, u is the x-velocity, v is the y-velocity, $E = \rho e = \frac{1}{2}\rho(u^2 + v^2)$ is the total energy, e is the internal energy of the gas, $p = (\gamma - 1)\rho e$ is the pressure, and γ is the ratio of specific heats. The associated relaxation system can be formulated as (4.23), where $\mathbf{a}^2 = \mathrm{diag}(a_1^2, a_2^2, a_3^2, a_4^2)$ and $\mathbf{b}^2 = \mathrm{diag}(b_1^2, b_2^2, b_3^2, b_4^2)$.

The eigenvalues of the Jacobian matrix $\mathbf{f}'(\mathbf{u})$ (or $\mathbf{g}'(\mathbf{u})$) are $\lambda_1 = u - c$, $\lambda_2 = \lambda_3 = u$ and $\lambda_4 = u + c$ (or $\mu_1 = v - c$, $\mu_2 = \mu_3 = v$ and $\mu_4 = v + c$). These are the characteristic speeds for one-dimensional gas dynamics and are needed here only for the estimation of relaxation variables. Thus, in all our numerical tests with

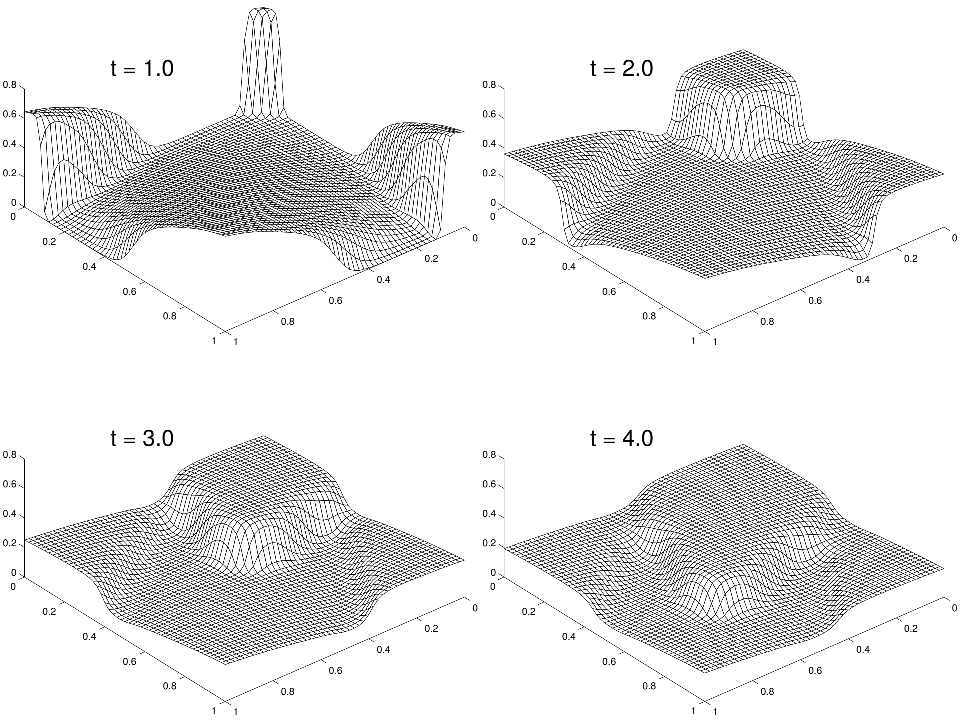

Fig. 6. Results for the inviscid two-dimensional Burger's equation (5.34).

equations (4.22)-(5.35) we used

$$\begin{aligned} a_1^2 = a_2^2 = a_3^2 = a_4^2 &= \max\Big(\sup|u-c|, \sup|u|, \sup|u+c|\Big), \\ b_1^2 = b_2^2 = b_3^2 = b_4^2 &= \max\Big(\sup|v-c|, \sup|v|, \sup|v+c|\Big). \end{aligned} \tag{5.36}$$

The following test examples are chosen:

The shock reflection problem. This problem was solved in [9] using the second order relaxation scheme. In our computations we take the same parameters as in [9]. Thus, the computational domain $\Omega = [0,4] \times [0,1]$; initially the domain Ω is filled by a free-stream supersonic inflow with Mach number 2.9. The Dirichlet boundary conditions are imposed at left and upper boundaries as

$$\begin{aligned} \mathbf{u}(0, y, t) &= (1, 2.9, 0, 5.99071)^T, \\ \mathbf{u}(x, 1, t) &= (1.69997, 4.45279, -0.86074, 21.30317)^T. \end{aligned}$$

The bottom boundary is a reflecting wall and the supersonic outflow condition is applied along the right boundary. The simulation is performed until $t = 5$ using $\Delta t = 0.005$. Plots of the pressure are shown in figure 7 using 30 equi-distributed contours on two different meshes. As can be seen from this figure, the reflected shock was very well captured by the relaxing scheme.

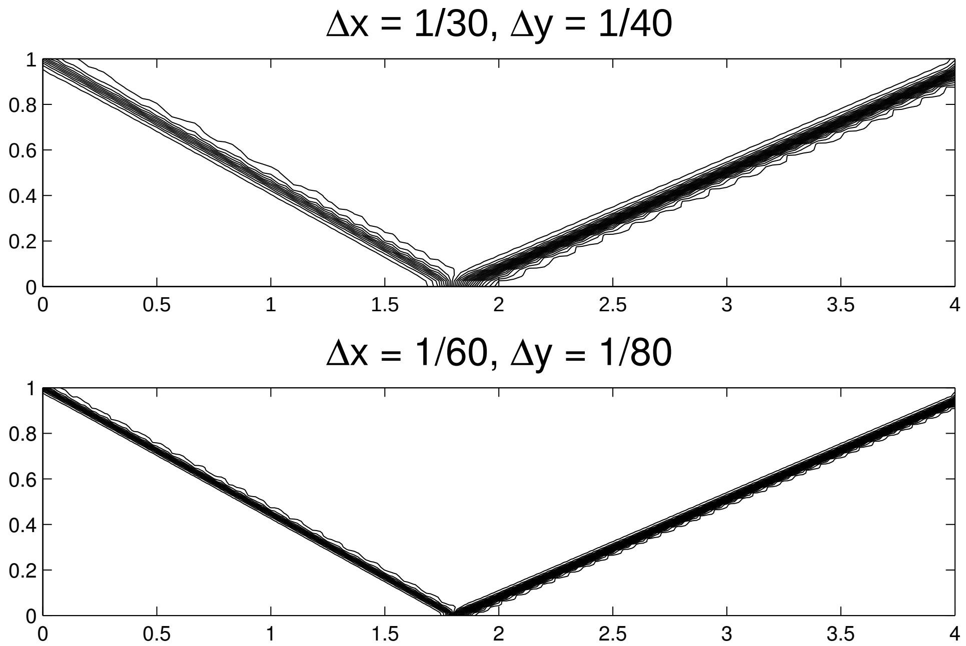

Fig. 7. Pressure contours for the shock reflection problem on two different meshes.

The double Mach reflection problem. This test example consists of the canonical double Mach reflection problem [20]. The spatial domain $\Omega = [0,4] \times [0,1]$. The reflecting wall lies at the bottom of the computational domain starting from $x = \frac{1}{6}$. Initially a right-moving Mach 10 shock is positioned at $x = \frac{1}{6}$, $y = 0$ and makes a $60°$ angle with the x-axis. For the bottom boundary, the exact post-shock condition is imposed for the part from $x = 0$ to $x = \frac{1}{6}$ and a reflective boundary condition is used for the rest. At the top boundary of the domain Ω, the flow values are set to describe the exact motion of the Mach 10 shock. Figure 8 shows 30 equi-distributed contour plots of the density at time $t = 0.2$ with $\Delta t = 0.0005$ on two different uniform meshes. We note that there is a very strong increase in resolution as the grids are refined due to the high order accuracy of the relaxation scheme. We can also see the complicated structures being captured by the new relaxing scheme.

The forward facing step problem. This is again a standard test problem for numerical schemes in two-dimensional Euler equations of gas dynamics (5.35). The setting of the problem is the following [20]: A right going Mach 3 uniform flow enters a wind tunnel of 1 unit wide and 3 units long. The step is 0.2 units high and is located 0.6 units from the left hand end of the tunnel. The problem is initialized by a

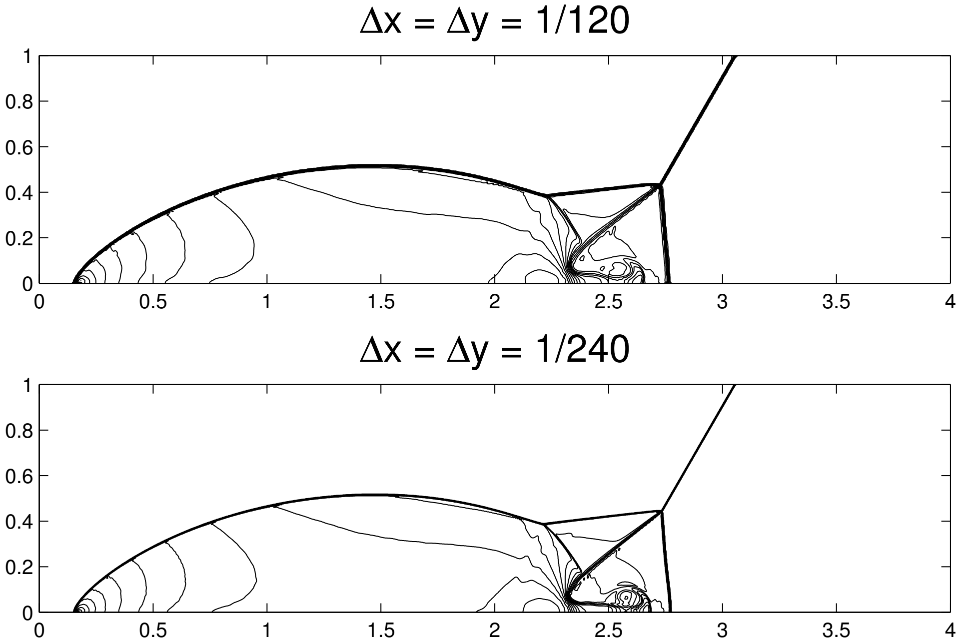

Fig. 8. Density contours for the double Mach reflection problem on two different meshes.

uniform, right going Mach 3 flow. Reflective boundary conditions are applied along the walls of the tunnel and inflow and outflow boundary conditions are applied at the entrance and the exit of the tunnel, respectively.

The corner of the step is a singularity, which has to be treated carefully in numerical experiments. Unlike in [20] and many other papers, we do not modify our relaxation scheme near the corner. However, we use different grid refinements to decrease the entropy layer at the downstream bottom wall. In figure 9 we show 30 equi-distributed contour plots of the density at time $t = 4.0$ using two different uniform meshes. We can clearly see that the resolution in the solution improves and the artifacts caused by the corner decrease as long as the gridpoints on the mesh increase.

6. Conclusion

We have presented a numerical scheme that is a generalization for relaxation methods. This scheme is easy to implement and above all no Riemann solvers are necessary. A third-order extension of this scheme is presented and tested. A marked improvement of the relaxation scheme is achieved. A few suggestions have been made on the choices of the matrices **A** and **B**. A rigorous result of how this can be done is still not available. We have further demonstrated that the relaxation formulation can be used as a platform for developing schemes for hyperbolic conservation

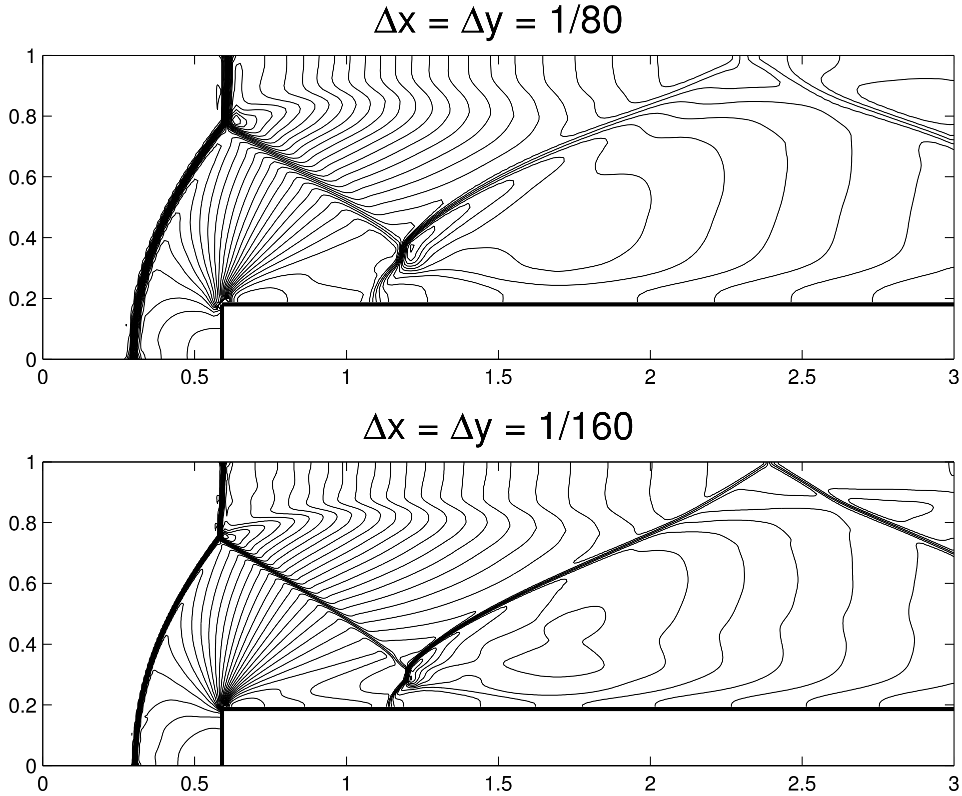

Fig. 9. Density contours for the forward facing step problem on two different meshes.

laws.

Acknowledgment

This work was supported by DAAD under grant A/99/04489 for the first author and DFG grant KL 1105/9-1 for the second author. The authors are deeply grateful to A. Klar, for his valuable suggestions and comments.

References

1. D. Aregba-Driollet and R. Natalini, *Convergence of relaxation scheme for conservation laws*, *Appl. anal.* **61** (1996) 163–193.
2. U. Ascher, S. Ruuth and R. Spiteri, *Implicit-explicit Runge-Kutta methods for time-dependent partial differential equations*, *AAppl. Numer. Math.* **25** (1997) 151–167.
3. M.K. Banda, A. Klar, L. Pareschi, and M. Seaïd *Lattice-Botzmann type relaxation systems and higher order relaxation schemes for the incompressible Navier-Stokes equation*, Submitted.

4. A. Chalabi, *Convergence of relaxation scheme for hyperbolic conservation laws with stiff source terms*, *Math. Comput.* **68** (1999) 955–970.
5. G.Q. Chen, C.D. Levermore and T.P. Liu, *Hyperbolic conservation laws with stiff relaxation terms and entropy*, *Comm. Pure Appl. Math.* **47** (1994) 787–830.
6. C.W. Shu and S. Osher, *Efficient Implementation of Essentially Non-Oscillatory Shock-Capturing Schemes*, *J. Comp. Phys.* **77** (1988) 439–471.
7. H. Fan, S. Jin and Z. Teng, *Zero Reaction Limit for Hyperbolic Conservation Laws with Source Terms*, *J. Diff. Equations* **168** (2000) 270–294.
8. S. Gottlieb, C.W. Shu and E. Tadmor, *Strong Stability-Preserving High-Order Time Discretisation Methods*, *SIAM Review.* **43** (2001) 89–112.
9. S. Jin and Z. Xin, *The Relaxation Schemes for Systems of Conservation Laws in Arbitrary Space Dimensions*, *Comm. Pure Appl. Math.* **48** (1995) 235–276.
10. S. Jin, *Runge-Kutta Methods for Hyperbolic Systems with Stiff Relaxation Terms*, *J. Comp. Phys.* **122** (1995) 51–67.
11. A. Klar, *Relaxation Schemes for a Lattice-Boltzmann type discrete velocity model and numerical Navier-Stokes limit*, *J. Comp. Phys.* **148** (1999) 1–17.
12. A. Kurganov and D. Levy, *A third-Order Semi-Discrete Central Scheme for Conservation Laws and Convection-Diffusion Equations*, *SIAM J. Sci. Comp.* **23** (2000) 1461–1488.
13. A. Kurganov and E. Tadmor, *New High-Resolution Central Schemes for Nonlinear Conservation Laws and Convection-Diffusion Equations*, *J. Comp. Phys.* **160** (2000) 241–282.
14. C. Lattanzio and D. Serre, *Convergence of a relaxation scheme for hyperbolic systems of conservation laws*, *Numer. Math.* **88** (2001) 121–134.
15. D. Levy, G. Puppo and G. Russo, *Compact Central Schemes for Multidimensional Conservation Laws*, *SIAM J. Sci. Comp.* **22** (2000) 656–672.
16. H.L. Liu and G. Warnecke, *Convergence rates for relaxation schemes approximating conservation laws*, *SIAM J. Numer. Anal.* **37** (2000) 1316–1337.
17. R. Natalini, *Convergence to equilibrium for relaxation approximations of conservation laws*, *Comm. Pure Appl. Math.* **49** (1996) 795–823.
18. L. Pareschi and G. Russo, *Implicit-Explicit Runge-Kutta Schemes for Stiff Systems of Differential Equations*, *Recent Trends in Numerical Analysis, Edited by L.Brugnano and D.Trigiante* **3** (2000) 269-289.
19. B. Van Leer, *Towards the Ultimate Conservative Difference Schemes V. A second-Order Sequal to Godunov's Method*, *J. Comp. Phys.* **32** (1979) 101–136.
20. P. Woodward and P. Colella, *The Numerical Simulation of Two-Dimensional Fluid Flow with Strong Shocks*, *J. Comp. Phys.* **54** (1984) 115–173.
21. W.Q. Xu, *Relaxation limit for piecewise smooth solutions to conservation laws*, *J. Diff. Eq.* **162** (2000) 140–173.
22. G. Sod, *A survey of several finite difference methods for systems of nonlinear hyperbolic conservation laws*, *J. Comp. Phys.* **27** (1978) 1–31.
23. P. D. Lax, *Weak solutions of nonlinear hyperbolic equations and their numerical computation*, *Comm. Pure Appl. Math.* **7** (1954) 159–193.